Conf-940723--43

UCRL-JC-118120
PREPRINT

Laser Properties of an Improved Average-Power Nd-Doped Phosphate Glass

S. A. Payne
C. D. Marshall
A. J. Bayramian
G. D. Wilke
J. S. Hayden

This paper was prepared for submittal to the SPIE Proceedings
on Properties and Characteristics of Optical Glass III
San Diego, CA
July 24–29, 1994

March 15, 1995

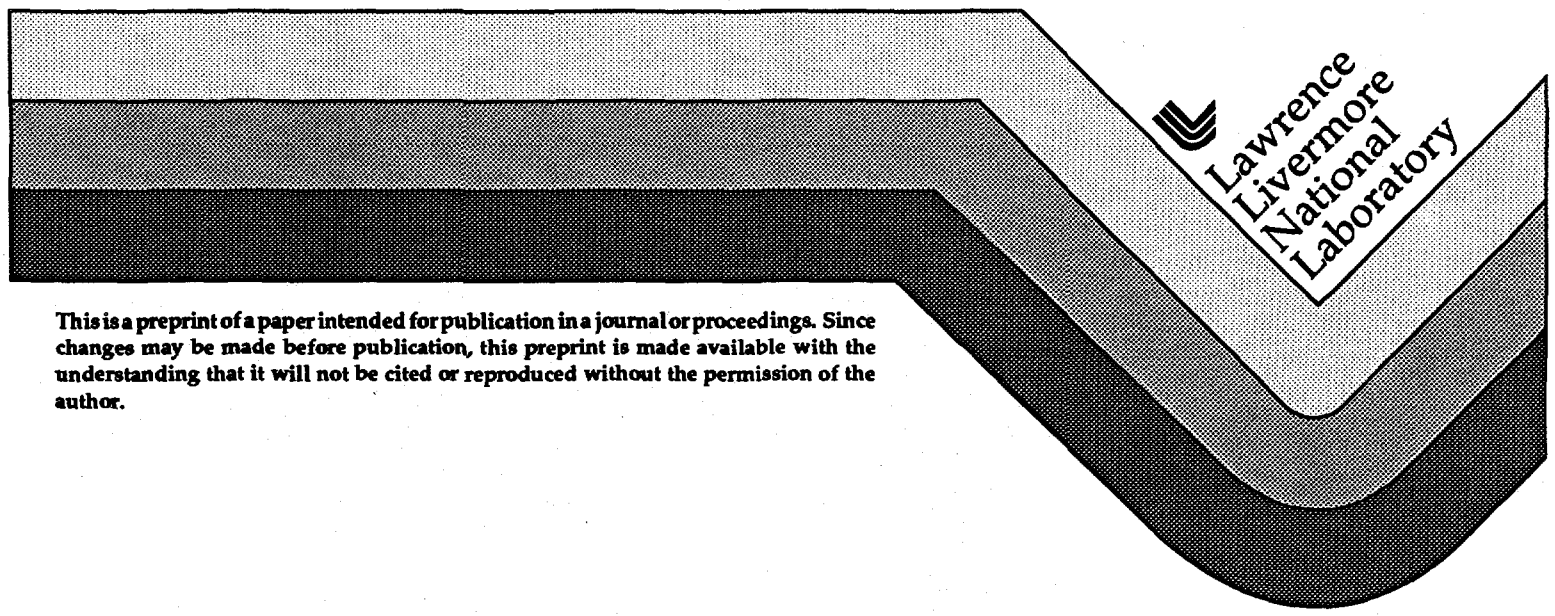

DISCLAIMER

Portions of this document may be illegible in electronic image products. Images are produced from the best available original document.

Laser properties of an improved average-power Nd-doped phosphate glass

Stephen A. Payne, Christopher D. Marshall, Andrew J. Bayramian, and Gary D. Wilke

Lawrence Livermore National Laboratory, University of California
Livermore, California 94550

Joseph S. Hayden

Schott Glass Technologies, Inc.
Duryea, Pennsylvania 18642

ABSTRACT

The Nd-doped phosphate laser glass described herein can withstand 2.3 times greater thermal loading without fracture, compared to APG-1 (commercially-available average-power glass from Schott Glass Technologies). The enhanced thermal loading capability is established on the basis of the intrinsic thermomechanical properties (expansion, conduction, fracture toughness, and Young's modulus), and by direct thermally-induced fracture experiments using Ar-ion laser heating of the samples. This Nd-doped phosphate glass (referred to as APG-t) is found to be characterized by a 29% lower gain cross section and a 25% longer low-concentration emission lifetime.

1. INTRODUCTION

Nd-doped glasses have been deployed for 1.05 μm laser systems for several decades now, and scientists have come to understand how the properties of these glasses impact the laser performance. The first use of a Nd-doped glass was reported by Snitzer in 1961, when he demonstrated that laser action was feasible.[1] Over the years, Nd:glass-based systems have tended to involve lasers dedicated to generating high single-shot energies, high average power, or ultrashort pulses. All three of these areas have continued to experience intense interest to the present day. For example, the early short-pulse systems entailed picosecond passively mode-locked Nd:glass lasers based on Q-switch dyes.[2] Most recently Keller and coworkers have shown that it is possible to operate femtosecond-type sources with quantum-well mirrors and Kerr lens mode-locking.[3] High energy (psec and nsec) pulsed Nd:glass lasers have been utilized predominantly for plasma physics and inertial confinement fusion experiments.[4] Continuing interest in this area has led to lasers evolving from ~1 kJ to 100 kJ — these systems are anticipated to reach the megajoule class within the next decade. Lastly, high average power Nd:glass lasers now operate at about 100 watts,[5] and are expected to attain the kilowatt level in the future. The general situation is that Nd:glass is a technologically important means of generating laser radiation near 1.05 μm, and great interest in this laser material will persist into the foreseeable future.

An important step in laser glasses occurred in 1967 when phosphate-based glass compositions were first explored.[6] Phosphates were found to have several important attributes over silicate glasses.[7] In particular, Nd:phosphate glasses provide greater extraction efficiency[8] (by virtue of reduced hole-burning and a higher gain cross section), and can also be manufactured free of platinum inclusions[9] (thereby greatly increasing the optical damage threshold). Since micron-size platinum inclusions appear to be an inevitable consequence of today's glass melting technology, it is of crucial significance to note that it is possible to chemically treat phosphate glasses so as to completely eliminate these particles. It has not yet been possible to achieve comparable results for silicates or fluorides. As a consequence, Nd:phosphate glasses are generally regarded as the medium of choice for most bulk laser applications. It is also practical to fabricate Nd:phosphate glasses in large size (40 cm aperture) and with excellent optical quality (loss of <0.2%/cm).

If we proceed with the assumption that phosphates are the preferred medium for most (non-fiber) Nd:glass laser applications, then one is compelled to evaluate the range of properties available from this class of materials. In this article we discuss our research on the development of phosphate glasses that offer an enhanced thermal fracture limit. Among the laser glasses in common usage are LG-750 and APG-1 (from Schott Glass Technologies), in addition to Nd:phosphate glasses produced by Hoya,[10] Kigre[11] and other companies. The result of our campaign to define a Nd:glass with improved thermomechanical properties is the so-called APG-t glass, where "t" refers to "test-glass" since this glass is not yet commercially available. We describe the properties of APG-t in the context of the established characteristics of LG-750 (fusion laser glass) and APG-1 (average-power glass), in order to emphasize the uniqueness of the new glass discussed herein.

2. SPECTROSCOPIC PARAMETERS

The absorption spectrum appears in Fig. 1 where it is plotted on an absolute scale by correcting the optical density for the Nd concentration and sample length. The absorption spectrum is similar to that of many other Nd-doped phosphate glasses. The band near 800 nm (typically used for laser diode pumping) is a result of the $^4I_{9/2} \rightarrow {}^4F_{5/2}, {}^2H_{9/2}$ transitions. Upon excitation of the Nd absorption bands pictured in Fig. 1, four emission bands are induced. Our primary interest is focused on the band peaked near λ_p = 1054 nm. The result of exciting the sample with a Xe lamp and monitoring the emission with a PbS detector/monochromator combination is displayed in Fig. 2 (after being corrected for the spectral response function). The emission width, defined as

$$\Delta\lambda_{em} = \frac{\int I_{em}(\lambda)\, d\lambda}{I_{em}(\lambda_p)} \quad , \tag{1}$$

is found to be $\Delta\lambda_{em}$ = 31.5 nm for APG-t. The peak emission cross section may be calculated with the Einstein relation[12]:

$$\sigma_{em}(\lambda_p) = \frac{\beta_{11/2}\,\lambda_p^4}{8\pi n^2 c \tau_{rad} \Delta\lambda_{em}} \tag{2}$$

where the refractive index (n = 1.511), $^4F_{3/2} \rightarrow {}^4I_{11/2}$ branching ratio $\beta_{11/2}$, and the radiative lifetime τ_{rad} are required.

One way to determine $\beta_{11/2}$ and τ_{rad} is to use the theory of Judd and Ofelt (JO).[13] Here, the oscillator strengths of the Nd^{3+} absorption bands observed in Fig. 1 are first evaluated and then, based on the identity of the electronic states and symmetry arguments, the calculation of each band may be reduced to a simple linear combination of the three so-called JO parameters. For the case of APG-t they are (in units of 10^{-20} cm^2): $\Omega_2 = 5.60$, $\Omega_4 = 4.02$, and $\Omega_6 = 4.22$. We are also able to calculate the radiative lifetime of the $^4F_{3/2}$ state by summing the transition strengths to all of the ^4I_J ground state levels, yielding τ_{rad} (JO) = 451 ± 20 μsec (average of four samples). By similar means we can use the JO theory to determine that the fractional emission into the $^4F_{3/2} \rightarrow {}^4I_{11/2}$ transition (compared to all the ^4I_J) is $\beta_{11/2} = 0.480$.

Since τ_{rad} (JO) is derived solely from the absorption spectra, we also evaluate the radiative lifetime by a second, more direct method. In these experiments, we obtained the emission lifetime (τ_{em}) as well as a measurement of the quantum yield (η_{QY}) in order to provide an independent assessment of the radiative lifetime using[14]

$$\tau_{rad}(QY) = \tau_{em} / \eta_{QY} \tag{3}$$

The quantum yield was measured with the aid of an integrating sphere, and broadly detecting the 880 nm, 1050 nm and 1300 nm emissions with a PbS diode. The incoherent output from an Ar ion laser

pumped Ti:sapphire crystal served as the excitation source, and a sample of LG-750 with a known quantum yield was employed to establish an absolute calibration for the system.[15] The average radiative lifetime deduced by this method is τ_{rad} (QY) = 455 ± 30 μsec. Accordingly, we employed the average of the JO and QY values in (2), or τ_{rad}= 453 μsec, to find that the peak emission cross section is $\sigma_{em}(\lambda_p)$ = 2.39×10^{-20} cm^2.

A well-known issue impacting all Nd-doped materials is that of concentration quenching.[16] In this effect, the situation initially entails two Nd^{3+} ions where one is excited in the $^4F_{3/2}$ state, while the other is in the $^4I_{9/2}$ ground state. Then the ions cross relax such that they are both converted to the $^4I_{15/2}$ level, followed by nonradiative decay back to the ground state. This phenomenon becomes enhanced at higher concentrations since the Nd ions interact more strongly. In order to characterize the concentration quenching, we examine the emission lifetimes of samples with various Nd concentrations. The measured lifetimes τ_{meas} had to be corrected for two additional effects, including radiation trapping and water quenching.[14,15,16] After applying these two corrections to derive the emission lifetime purely influenced by concentration quenching, we may plot τ_{em} versus the Nd concentration N_{Nd} in units of 10^{20} cm^{-3}, as shown in Fig. 3. Here, similar data acquired for the commercial laser glasses APG-1 and LG-750 are included for comparisons; the radiative lifetimes (see above) are plotted to describe the zero concentration limit. The APG-t data points of Fig. 3 are observed to fall on a simple straight line. In lieu of analyzing the data on the basis of theories requiring fitting to several parameters,[15] we employ an empirical linear approach with

$$\tau_{em} = \tau_0 (1 - N_{Nd}/q) \qquad (4)$$

for $N_{Nd} \lesssim q/2$, and obtain τ_0 = 464 μsec and $q = 10.6 \times 10^{20}$ cm^{-3}.

Having now completed our discussion of the emission bandwidth, radiative lifetime, cross section and quenching, a summary of these data is provided in Table 1. The data concerning LG-750 and APG-1 are treated in an equivalent manner so that they may be directly compared with APG-t. From Table 1 it is apparent that APG-t is characterized by a cross section σ_{em} that is ~29% lower than APG-1. APG-t also differs in that the low-concentration lifetime τ_0 is increased ~25%, while the quenching curve is somewhat steeper (i.e., smaller q value). The refractive index, Abbe' number, and change of refractive index with temperature are listed in Table 1 for completeness.

3. THERMAL FRACTURE LIMIT

The ability of a phosphate laser glass to sustain internal thermal gradients without fracture is an important characteristic for high average power applications. The primary predicted advantage of APG-t over other phosphate glasses is its superior thermal and mechanical properties. In an effort to experimentally establish the expected superior thermal properties of APG-t, an experiment was devised that would demonstrate the fracture probability in the presence of thermal gradients. Nd-doped APG-t, APG-1 and LG-750 laser glasses containing 3.5%, 3.43%, and 4.0% by weight, respectively, were fabricated into ~3 x 3 x 3 mm cubes (~10 for each glass type) with laser quality polishes on two opposing sides. These glass samples were then irradiated with 514 nm light from an argon-ion laser. The argon-ion beam was variably attenuated (0 to 5W) and focused with a 7.5 cm focal length lens to a 40 μm diameter (1/e) near-Gaussian spot size. The samples were tested by first starting out at relatively low 514 nm power levels and then translating each sample back and forth across one transverse dimension and observing whether catastrophic cracking occurred. The beam power was then increased in small incremental steps with similar sample translations being performed between each step. When fracture was observed, the incident power was recorded. This procedure was repeated for each of the samples. It is relevant to note that the cracking appeared to originate from the surface and to propagate into the bulk of the material.

The deposited thermal power density, P_{th}/V, was calculated by including the optical absorption fraction, surface reflection, and the fraction of optical power that is nonradiative (i.e., leading to heating), which becomes

$$P_{th}/V = \frac{P_{inc}\{1 - \exp(-\alpha\ell)\}\{1 - R\}\{1 + R\exp(-\alpha\ell)\}}{\pi r_0^2/\alpha}\left\{1 - \left(\frac{\tau_{em}}{\tau_0}\right)\left(\frac{\lambda_{pump}}{\lambda_{em}}\right)\right\} \quad (5)$$

where the absorption coefficient at 514 nm, the sample length, the 1/e beam radius, and the Fresnel reflection coefficient are described with α, ℓ, r_0 and R, respectively, and were independently determined. The last term in brackets describes the fraction of the absorbed optical power that becomes thermal energy, including the quantum defect $\lambda_{pump}/\lambda_{em}$, and the ratio of the low concentration lifetime τ_0 to the measured lifetime τ_{em} (which is shorter due to concentration quenching). The fracture probability was determined by ranking the glasses in order of the thermal power density at which they fractured and assigning a fracture probability via the relation[17,18]

$$\Phi = (n - 0.5)/N \quad (6)$$

where n is the rank and N is the total number of samples of each glass type. The data appears in this format in Fig. 4, where the solid lines are numerical fits using Wiebull statistics that will be discussed in more detail later in this section.

The data clearly shows that LG-750 tends to fracture at lower thermal power density than is the case for APG-1, as one would expect from previous thermal-mechanical studies,[19] while APG-t exhibits a lower thermal fracture probability than APG-1 for a given thermal power density. Although only one sample of APG-t was observed to crack under thermal loading, there were eight other samples that were subjected to >100 kW/cm^3 for which no fracture was observed. Instead, a red line coincident with the laser illumination spot was observed, indicating that the sample had melted. Thus it was not possible to thoroughly "fracture test" these samples since the failure mode often entailed melting rather than cracking. The result nevertheless highlights the robustness of APG-t in that, at least for 40 μm spot size illumination, the glass melts before it was found to fracture.

Wiebull statistics can be employed to describe thermally induced fracture for samples with a given distribution of surface flaw sizes determined primarily by the surface polish technique. The absolute magnitude of the fracture probability scales with the sample size. As a consequence, larger samples are more likely to have a sufficiently large flaw to induce cracking at a particular irradiance than are small samples. Therefore, this treatment is most applicable for use in comparing samples of similar surface preparations and of a constant size. Although the details of this approach have been previously described, a brief outline will be presented here for completeness.[17,18] This treatment assumes that the sample cracks when the weakest point (corresponding to the location with the largest flaw) of the sample fails. The fracture probability for a two parameter Wiebull distribution can then be written as[20,21]

$$\Phi = 1 - \exp\left[-\left(\frac{\rho}{\rho_0}\right)^m\right] , \quad (7)$$

where m and ρ_0 are the adjustable shape and scaling parameters and ρ is the thermal power density expressed in units of power per unit volume. A least squares fitting routine was utilized for each of the three glass types to relate the data in Fig. 4 to the two adjustable parameters in Eq. 7. The scaling parameter, ρ_0, was varied independently for each sample since this parameter is expected to be proportional to the intrinsic ability of the glass to withstand fracturing. The shape parameter, m, was held constant between samples since this parameter is related to the distribution of flaw sizes left behind after polishing and all of the sample surfaces were prepared with the same polishing technique. The sum of the least squares errors of the three glass types was minimized. A value of 4.0 was found to simultaneously provide the best fit to the shape of the APG-1 and LG-750 data sets. The scaling parameters, ρ_0, then become 31.7 ± 1.3, 78.4 ± 0.9, and 210 ± 50 kW/cm^3 for LG-750, APG-1 and APG-t, respectively. The results of this analysis are shown as solid lines in Fig. 4 using Eq. 7 and the above parameter values. It is

noteworthy that the ρ_0 values only change by a few percent when m is varied by up to ±25% for LG-750 and APG-1, which shows that the ρ_0 fitting is robust.

The question naturally arises as to whether the scaling parameter, ρ_0, is proportional to what one would expect from theoretical predictions of the thermal shock parameter R_T, calculated from other measured material properties. The thermal shock parameter serves as a thermal figure of merit for high average power applications, and is directly related to the maximum thermal load which a surface cooled laser slab can withstand without fracture. It is expressed as[18]

$$R_T = \frac{K_{1c}\kappa(1-\nu)}{\alpha_{exp} E\sqrt{a}} \tag{8}$$

where K_{1c}, κ, ν, α_{exp}, E, and a are the fracture toughness, thermal conductivity, Poisson's ratio, thermal expansion coefficient, Young's modulus, and the radius of the damage initiating flaw size, respectively. Experimental values of the thermomechanical parameters are given in Table II for APG-t, APG-1 and LG-750.[19] By assuming a flaw size of $2a \approx 50$ μm which is typical for mechanically polished surfaces,[18] one obtains thermal shock parameters of 255, 111, and 46 W/m for APG-t, APG-1 and LG-750, respectively. The first two rows of Table II give the experimentally evaluated fracture scaling (i.e., derived from Fig. 4) along with the calculated thermal shock parameters, normalized to the values of LG-750 in both cases to aid in comparison. It is readily apparent that the thermal shock parameter (R_T) is proportional to the fracture scaling parameter (ρ_0) to within the error bars. Consequently, we believe that the above fracture experiments, which indicate that APG-t is significantly more fracture resistant than currently available high average power phosphate glasses such as APG-1, are validated by agreement with thermal shock parameter calculations. In this way, our somewhat tenuous fit through a single point in Fig. 4 has been validated on the basis of the inherent thermomechanical properties of the glasses.

4. SUMMARY

APG-t appears to be a viable Nd-doped phosphate glass that offers a new combination of laser, optical, thermal, and mechanical properties. In comparing APG-t to two other glasses that are commercially available from Schott Glass Technologies (LG-750 and APG-1), it becomes apparent that various trade-offs among the material properties are possible. For example, APG-t has a lower emission cross section σ_{em} and reduced extraction limit η_{ext}, although the thermal shock parameter R_T is substantially enhanced. Similarly, the concentration quenching is steeper for APG-t while the zero-concentration lifetime is longer (permitting greater energy storage for lightly-doped samples).

5. ACKNOWLEDGMENTS

We wish to thank Laura DeLoach for the measurements of the refractive indices, Ron Vallene and Peter Thelin for polishing the samples, and Lloyd Hackel for his support and encouragement during the course of this work (all of LLNL). We wish to thank Mary Kay Aston and Dave Sapak of SGT for their help in defining the composition of APG-t and for their insights into the properties of the glass in a production facility. This work was performed under the auspices of the U.S. Department of Energy by Lawrence Livermore National Laboratory under Contract No. W-7405-ENG-48 and additional support received from the ARPA Advanced Lithography Program.

6. REFERENCES

1. E. Snitzer, Phys. Rev. Lett. 7, 444 (1961).
2. A Lambereau and W. Kaiser, Opto-electronics 6, 1 (1974).
3. U. Keller, T. H. Chiu, and J. F. Ferguson, Opt. Lett. 18, 1077 (1993).
4. See, for example, E. M. Campbell, Phys. Fluids B 4, 3781 (1992).

5. J. L. Miller, C. B. Dane, L. Zapata, L. Hackel, and J. Abate, "Neodymium:glass zigzag slab regenerative amplifier laser system for x-ray lithography," in Conference on Lasers and Electro-Optics, vol. 12 of OSA Technical Digest Series (Optical Society of America, Washington, DC, 1992), p. 90.
6. O. Deutschbein, C. Pautrat and I. M. Svirchevsky, Rev. Phys. Appl. 1, 29 (1967).
7. L. M. Cook, A. J. Marker III, and S. E. Stokowski, in Proc. SPIE, vol. 505 (Soc. Photo-Optical Inst. Engineers, Bellingham, Washington, 1984) p. 102.
8. W. E. Martin and D. Milam, IEEE J. Quantum Electron. QE-18, 1155 (1982).
9. J. H. Campbell, E. P. Wallerstein, J. S. Hayden, D. L. Sapak, D. E. Warrington, A. J. Marker III, H. Toratani, H. Meissner, S. Nakajima, and T. Izumitani, Elimination of Platinum Inclusion in Phosphate Laser Glasses, May 26, 1989, UCRL-53922, Distribution Category UC-712 (available from National Technical Information Service, U.S. Department of Commerce, 5285 Port Royal Rd., Springfield, VA 22181).
10. Examples of common Nd-doped phosphate glasses include LHG-8, LHG-5, LHG-80 and HAP-3; Hoya Optics, Inc., 3400 Edison Way, Fremont, CA 04538.
11. Examples of common Nd-doped phosphate glasses include Q-88, Q-89, Q-98 and Q-100; Kigre, Inc., 100 Marshland Rd., Hilton Head Island, SC 29926.
12. W. Koechner, Solid State Laser Engineering, (Springer, New York, 1986), p. 17.
13. S. A. Payne, J. A. Caird, L. L. Chase, L. K. Smith, N. D. Nielsen, and W. F. Krupke, J. Opt. Soc. Am. B 8, 726, (1991).
14. S. A. Payne, M. L. Elder, J. H. Campbell, G. D. Wilke, M. J. Weber, and Y. T. Hayden, Ceramic Transactions 28, 253 (1992).
15. J. A. Caird, A. J. Ramponi, and P. R. Staver, J. Opt. Soc. Am. B 8, 1391 (1991).
16. H. G. Danielmeyer, M. Blätte, and P. Balmer, Appl. Phys. 1, 269 (1973).
17. J. E. Marion, J. Appl. Phys. 60, 69 (1986).
18. W. F. Krupke, M. D. Shinn, J. E. Marion, J. A. Caird, and S. E. Stokowski, J. Opt. Soc. Am. B 3, 102 (1986).
19. Schott Laser Glass Brochure 2303/90, Schott Glass Technologies, Inc., Duryea, PA (1990); ibid, 2302/91 (1991).
20. W. Wiebull, Royal Swedish Academy of Eng. Sci. Proc. 151, 1 (1939).
21. C. A. Johnson, in Fracture Mechanics of Ceramics, Vol. 5: Surface Flaws, Statistics and Microcracking, edited by R. C. Bradt, A. G. Evens, D. P. H. Hasselman, and F. F. Lange (Plenum, New York, 1983).

Table 1. Laser and optical parameters for three Nd-doped phosphate glasses.

Parameter	Symbol	Units	Value		
			APG-t	APG-1	LG-750
Emission peak	λ_p	nm	1054	1054	1054
Emission width	$\Delta\lambda_{em}$	nm	31.5	27.8	26.0
Radiative lifetime	τ_{rad}	μsec	456	361	347
Emission cross section	σ_{em}	10^{-20} cm^2	2.39	3.35	3.68
Quenching constants	τ_0	μsec	464	370	356
	q	10^{20} cm^{-3}	10.6	16.7	17.0
Refractive index	n_d	–	1.511 (a)	1.533	1.538
Abbé number	ν_d	–	67.8	67.9	66.3
Index change with temperature	dn/dT	10^{-6}/K	+4.0	+1.2	-5.1

(a) The Sellmeier dispersion formula is given as
$n^2 = 2.255122 + 0.009917/(\lambda^2 - 0.014835) - 0.009616\,\lambda^2$, where λ is in microns

Table II. Thermal and mechanical properties of APG-t, APG-1, and LG-750 phosphate glasses measured experimentally or taken from Ref. 19.

Parameter	Symbol	APG-t	APG-1	LG-750
Experimental Fracture Scaling Parameter normalized to LG-750	ρ_0/ρ_0 (LG-750)	6.6 ± 1.7	2.4 ± 0.2	1.0
Calculated Thermal Shock Parameter normalized to LG-750	R_T/R_T (LG-750)	5.5	2.4	1.0
Calculated Thermal Shock Parameter (using a = 25 μm)	R_T (W/m)	254	111	46
Thermal Conductivity	κ (W/mK)	0.86	0.85	0.51
Fracture Toughness	K_{1c} (MPa m$^{1/2}$)	0.80	0.60	0.40
Thermal Expansion Coefficient	α_{exp} (10^{-6}/K)	6.38	9.84	13.1
Young's Modulus	E (GPa)	64.4	71	50.0
Poisson's Ratio	ν (unitless)	assumed to be same as APG-1	0.24	0.256
Density	ρ (g/cm^3)	2.56	2.62	2.96
Glass Transition Temperature	T_g (K)	549	455	452

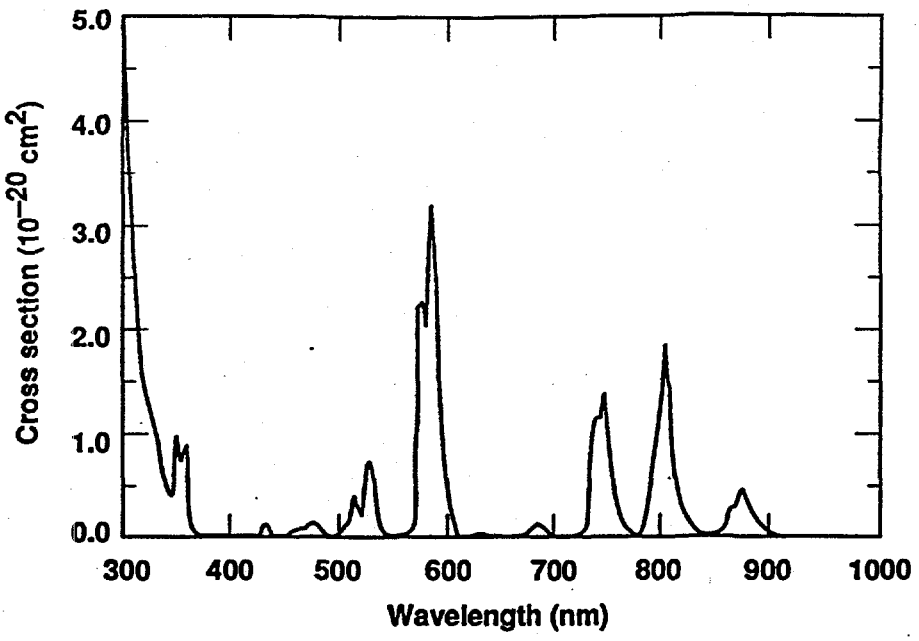

Figure 1: Absorption spectrum of APG-t glass plotted versus wavelength on an absolute cross section scale.

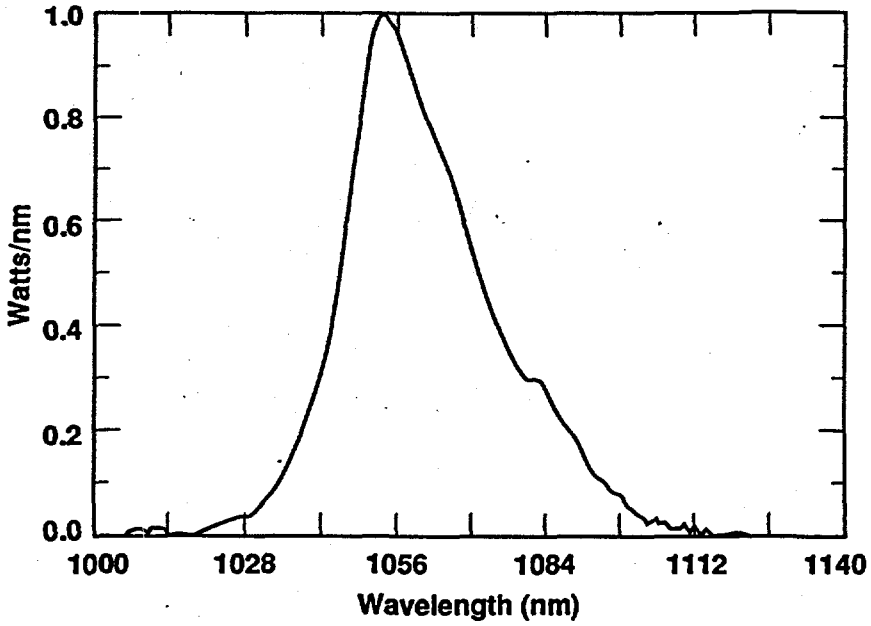

Figure 2: Emission spectrum of APG-t arising from the $^4F_{3/2} \rightarrow {}^4I_{11/2}$ transition.

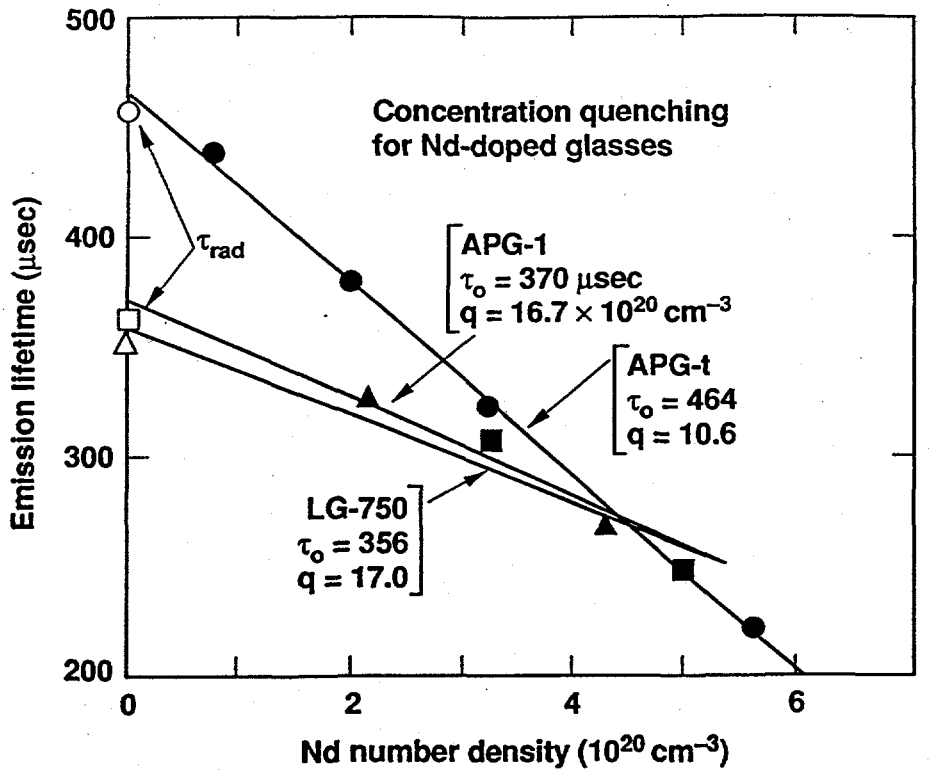

Figure 3: Plot of the Nd^{3+} emission lifetime as a function of dopant concentration for APG-t, APG-1 and LG-750.

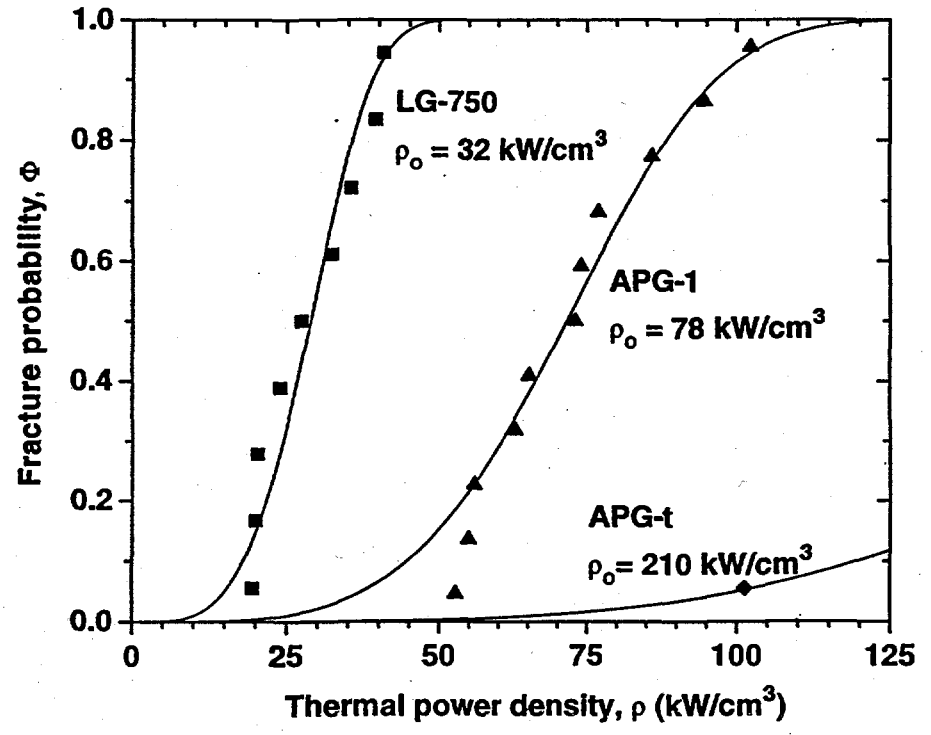

Figure 4: Thermal fracture results for APG-t, APG-1, and LG-750 glasses. The solid lines are numerical fits to the experimental data points using Wiebull statistics to describe the fracture probability.